UDC 535.341:666.265.1

LOCAL ELECTRIC FIELD ENHANCEMENT IN THE VICINITY OF Ag NANOPARTICLES AND THEIR AGGLOMERATES IN ZINC-PHOSPHATE AND SILICATE GLASS

V. V. Srabionyan,[1] M. P. Vetchinnikov,[2] D. S. Rubanik,[1] V. A. Durymanov,[1] I. A. Viklenko,[1] L. A. Avakyan,[1] E. M. Zinina,[2] G. Yu. Shakhgildyan,[2] V. N. Sigaev,[2] L. A. Bugaev[1]

Based on calculations, the spatial distribution of the local electric field (LEF) for various structural configurations of silver nanoparticles (NPs) in silicate and zinc-phosphate glasses was studied. The features of this distribution determine the efficiency of energy transfer from plasmonic NPs to rare earth (RE) ions located in the particle vicinity. The mechanism of energy transfer through field enhancement via surface plasmon resonance of particles, which is dominant for NPs of sizes of ≥ 5 nm, is determined by several factors. To clarify their roles and significance, the dependencies of LEF upon the size, spatial distribution, and degree of agglomeration of silver NPs in glass were studied. Comparative analysis of the nature of the field enhancement in places of hypothetical location of RE ions was carried out on the basis of a visual representation of the spatial distribution of the LEF in the vicinity of agglomerates of plasmonic NPs. Based on simulations, the dependencies of LEF intensity enhancement, the spatial distribution of such places in relation to the nearest plasmonic particle, upon the concentration of NPs, their size, degree of agglomeration, and the presence of small (≤ 5 nm) particles in the sample along with the relatively large ones, were determined. The optimal configuration of silver particles in glass for obtaining the maximum average enhancement of LEF intensity per the site of possible location of RE ion is revealed to be an agglomerate of NPs with sizes slightly larger than 25 nm and average distances between particle centers about 30 nm.

Keywords: surface plasmon resonance, silver nanoparticles and their agglomerates in glass, local electric field enhancement.

1. INTRODUCTION

Glasses containing metallic nanoparticles (NPs) are extensively studied in order to obtain composite materials with valuable optical properties [1 – 3]. Of particular interest are glasses with silver NPs due to well-defined localized surface plasmon resonance (LSPR) in the visible region of optical extinction spectra [4 – 12]. This phenomenon ensures the localization and preservation of incident light energy on a nanometer scale in space and on a femtosecond scale in time. One of the most significant and rapidly developing directions involves the use of LSPR in Ag NPs to develop laser-active

materials having improved luminescent characteristics. In particular, such materials can be used as effective light-sensitizing agents to enhance laser junctions on rare earth (RE) ions introduced into glass [13 – 18]. Based on numerous studies exploring the impact of noble metal NPs on the luminescent characteristics of RE ions, the primary mechanism is shown to involve the enhancement of the local electric field (LEF) due to the presence of LSPR in plasmonic NPs with RE ions located in the field enhancement regions [19 – 21]. This is shown to represent a primary mechanism for noble metal NPs having a size (D) exceeding 5 nm [20]. In addition, it has been established that the enhancement of LEF through LSPR can also occur for small Ag NPs with D of about 2 nm [22]. For the latter, the field enhancement effect can compete with various mechanisms of energy transfer,

[1] Southern Federal University (SFedU), Rostov-on-Don, Russia.
[2] Mendeleev University of Chemical Technology of Russia (MUCTR), Moscow, Russia.
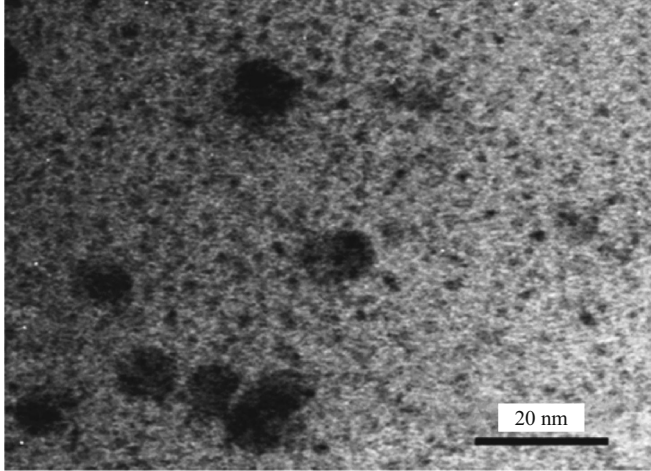
Fig. 1. TEM image of a glass sample containing an Ag NP following Ag$^+$ ↔ Na$^+$ ion exchange and subsequent irradiation with 5000 pulses by a UV laser.

both radiative and nonradiative, including energy transfer from multi-phonon relaxation due to the quantum dimensional effect [20] or Foerster resonant energy transfer [23 – 26].

The efficiency of sensitization of RE ions by LSPR of plasmonic NPs depends on a number of factors, chiefly:

1) the degree of energy overlap of the LSPR of particles and the absorption energies of RE ions capable of inducing resonance (pumping) [21, 27, 28];

2) the spatial size and localization of regions with enhanced LEF both near individual nanoparticles and their agglomerates;

3) the probability of RE ions being located within such spatial regions. The last two conditions, in turn, depend on the concentration and size of plasmonic NPs, the degree of their agglomeration, and the concentration of RE ions in glass. This concentration, however, should be less or equal to the experimentally determined upper limit for the content of RE ions, preventing the concentration quenching of their luminescence due to the reverse transfer of energy from RE ions to NPs [21, 29 – 31].

This paper presents a theoretical study of the LEF distribution or the number of photonic states N in the vicinity of both single monometallic silver NP and their agglomerates synthesized in a glass matrix [32 – 38], depending on the particle size, concentration, and degree of their agglomeration. The dielectric properties of the glass matrix were considered using the refractive index $n = 1.5$, corresponding to both silicate and zinc phosphate glasses. By using modeling for given concentrations and average sizes of plasmonic NPs in glass, the dependencies of the radial distribution of LEF enhancement sites relative to the surface of the average silver NPs were determined. The optimal synthesis conditions (concentrations of introduced plasmonic metals and RE ions, and glass treatment with temperature or laser irradiation to

form NP) proposed on the basis of these dependencies can ensure a high probability of RE ion localization near NP where LEF enhancement is significant.

2. MATERIALS AND CALCULATION METHODS

The areas of LEF enhancement in the vicinity of silver NPs and their agglomerates were calculated using the size and spatial distribution of Ag NPs in silicate glass, which was first subjected to ion exchange followed by irradiation with a UV laser (193 nm) with the number of pulses equal to 5000 [32]. The image of the Ag NP in such a glass is shown in Fig. 1.

The effect of the LEF induced by LSPR of plasmonic NPs on the fluorescence enhancement of RE ions located near such particles is interpreted using Fermi's golden rule. This rule defines the probability P of photoabsorption or pumping of RE ions surrounded by a LEF or a field of photons incident on RE ions, whose number N corresponds to the intensity of the LEF:

$$P_{i \to f} = \frac{2\pi}{\hbar} \left| \left\langle \Psi_f \left| V \right| \Psi_i \right\rangle \right|^2 \rho(E_{i \to f}). \qquad (1)$$

In this expression, $\rho(E_{i \to f})$ — density of photonic states around the RE ion with an energy corresponding to the transition of an electron in the RE ion from the initial level of the nucleus i with the wave function Ψ_i to the final state Ψ_f; and $\left\langle \Psi_f \left| V \right| \Psi_i \right\rangle$ — transition matrix element that occurred due to the influence of the perturbation potential V of exciting photons. Therefore, the final dependence has the form of $P_{i \to f} \sim N$; $\hbar$ — Planck constant.

The LEF calculations near single monometallic plasmonic nanoparticles and their agglomerates were carried out using two different approaches:

1) the T-matrix method implemented in the T-matrix multiple scattering software code [39] using the developed Python interface to the MSTM code [41, 42];

2) the numerical solution of Maxwell's equations by the finite difference method using the COMSOL Multiphysics software package [42].

In the second scenario, perfectly matching layers [43] were used to restrict the modeled "box" and suppress the reflection of waves from its boundaries, which are absent in the real material. The T-matrix method was used to identify and eliminate possible instabilities of the numerical solution for Maxwell's equations by the finite difference method implemented in COMSOL. On the other hand, the finite difference method allows the LEF to be investigated in infinite regular 1D and 2D arrays of plasmon NPs, where the T-matrix method fails to provide an accurate result.

As shown in the TEM image, the LEF calculations for plasmonic Ag nanoparticles distributed in a specific spatial arrangement were carried out for particle agglomerates. These agglomerates represent groups with a finite number of
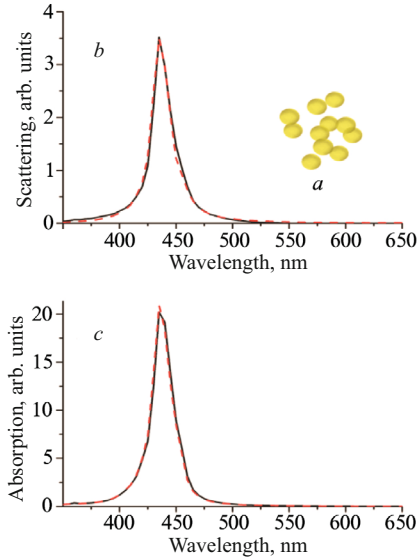
Fig. 2. Compared contributions of scattering (*b*) and absorption (*c*) to an extinction spectrum, calculated in COMSOL (solid black curve) and MSTM (dotted red curve) for Agglomerate-1 (*a*), which consists of 11 silver NPs with dimensions of $D = 10$ nm, located at a distance of $R_{ij} \geq 15$ nm relative to each other.

Fig. 3. Schematic representation of LEF distribution near silver NP agglomerate in the form of a "plane section" and $N/N_0\,(R)$ using an averaged dependence of LEF enhancement.

electromagnetically interacting particles, which should be taken into account for the theoretical characterization of the optical absorption spectra of plasmonic Ag NPs distributed in space [41]. The dielectric functions for the bulk silver material were taken from experimental data published elsewhere [44]. As shown in the work [15], the dielectric functions for silver nanoparticles smaller than 10 nm depend on the size. In order to address the impacts of the small size of nanoparticles below 10 nm, it is important to consider corrections to the calculated dielectric function. For nanoparticles with a size of 10 nm, such corrections were not applied in the present study: in this case, their values are insignificant in the visible range for the real part of the dielectric function responsible for photon scattering, while the difference between the imaginary parts of the calculated dielectric functions (responsible for absorption) for such NPs and for bulk silver is minimal at the LSPR wavelength (about 430 nm) [45]. However, the above-mentioned small difference in imaginary parts between the calculated dielectric functions for Ag nanoparticles with a size of 10 nm and for bulk silver at 430 nm has no effect on further findings about the relative variations of the LEF distribution near the considered diverse agglomerates of Ag NPs with a size of about 10 nm.

Figure 2 shows the results of a test calculation comparing the calculations of absorption and scattering contributions calculated using the MSTM and COMSOL software codes to the extinction spectrum of Agglomerate-1, which consists of 11 Ag NPs with the dimensions of $D = 10$ nm with the distance between their centers of $R_{ij} \geq 15$ nm.
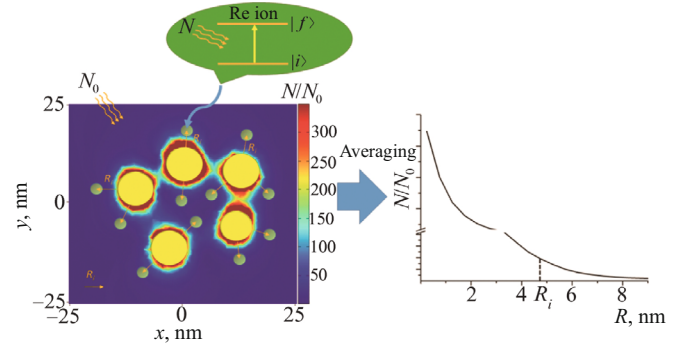
The proposed methodology for effectively analyzing the calculated spatial distributions of LEF near plasmonic nanoparticles and their agglomerates can be used to obtain one-dimensional dependencies of the average field enhancement on the distance to the surface of the nearest particle. By enhancing the average LEF falling at a hypothetical location of the RE ion in the immediate vicinity of the plasmonic agglomerate, the methodology facilitates quantitative characterization of the LEF for each of the possible local structural configurations of plasmonic NP systems. Recommendations on preferred nanoparticle type, optimal average size and spacing, and the optimal degree of agglomeration formulated on the basis of this data can be useful for the experimental preparation of state-of-the-art laser materials.

The proposed approach to determining the characteristics of LEF involves the following steps. In the first step, the LEF was calculated for each spatial point near the selected agglomerate of plasmonic NPs where a hypothetical RE ion could be located. The density of such points was selected to ensure monotonic LEF characteristics. In a subsequent step, rather than the conventional representation of the LEF intensity distribution cross plane cross-sections (which depends on their orientation relative to the directions of incidence, polarization of the external field, and their relative orientation to the NP agglomerate), the average LEF enhancement was analyzed across all potential RE ion positions. At that, the RE ions were located at equidistant points R_i from the nearest plasmonic NPs, in the range of $R_i \pm 0.25$ nm, with 0 on the axis of these distances R denoting the NP surfaces within the agglomerate. Fig. 3, schematically depicts the transition from plane section representation to the described depiction of LEF distribution via an averaged $N/N_0\,(R)$ dependency.

The plasmonic NPs and the associated spatial points used to calculate the LEF were adjusted to accommodate the periodicity of a cubic box. The given number of these points was evenly distributed within the volume of the corresponding regular cubic box. The distance distribution between RE ions and the nearest plasmonic NPs was determined using the Monte Carlo simulation method, which assumes an uncor-

related uniform distribution of hypothetical location points for the RE ions in a glass sample (Fig. 4*d*). The number of the spatial LEF calculation points and the size of the box were selected in such a way as to ensure the independence of the simulation from their values.

The number of possible location points of the RE ions as a function of the distance to the surface of the nearest NP was considered using histograms having a bin width of approximately 0.5 nm. The probability density was estimated as the ratio between the number of points in a specific bin at a given distance from the nearest NP, the bin width being divided by the total number of points in the box. The number of plasmonic NPs for LEF calculations was selected based on the concentration of Ag atoms reported in a previous study [32]. The sizes, locations, and degree of nanoparticle agglomeration were selected to replicate the structural configurations and sizes observed in the TEM image of the glass sample shown in Fig. 1 [32]. The formation of Ag nanoparticles in glass involved ion exchange ($Ag^+ \leftrightarrow Na^+$) followed by irradiation with 5000 UV laser pulses (wavelength 193 nm, pulse duration 20 nsec).

3. RESULTS AND DISCUSSION

Figure 1 shows the two main types of silver NPS formed:

1) NPs with a size of $D = 1 – 5$ nm randomly distributed throughout the sample with an average interparticle distance R_{ij} of approximately 10 nm;

2) NP with a size of $D = 8 – 15$ nm located at a distance R_{ij} of approximately 35 nm or closely grouped into the agglomerates with R_{ij} of approximately 15 nm.

In the present study, the different sizes and spatial distribution of Ag NPs represent possible types of deposition of nanoparticles in the glass matrix. This can have various effects on the luminescent properties of embedded RE ions due to the different spatial distribution of LEF near the agglomerates of plasmonic NP.

In order to establish the LEF distributions for the considered groups of silver nanoparticles conforming to the NPs observed in Fig. 1, the calculations in the MSTM program code were carried out using model agglomerates of $10 – 15$ NPs as reported in the work [41]. The wavelength λ of the incident light selected close to the wavelength of the LSPR maximum for each type of Ag NP agglomerates was in the range of $425 – 440$ nm depending on the considered particle size and their mutual arrangement.

Spatial distributions of LEF near Ag NP agglomerates were calculated for the following groups of particles:

1) Agglomerate-1: particle size of $D = 10$ nm and distances between particles $R_{ij} \geq 15$ nm (values in the lower left part of the TEM image in Fig. 1);

2) Agglomerate-2: $D = 10$ nm, $R_{ij} \geq 12$ nm (lower left corner in Fig. 1);

3) Agglomerate-3: small particles with $D = 5$ nm and $R_{ij} \geq 10$ nm (upper right corner in Fig. 1);

4) Agglomerate-4: $D = 15$ nm, $R_{ij} \geq 35$ nm (center of the upper part in Fig. 1), without the small Ag particles located around the large particles;

5) Agglomerate-5: the same large particles as in Agglomerate-4 ($D = 15$ nm, $R_{ij} \geq 35$ nm) surrounded by small Ag NPs with $D = 5$ nm and $R_{ij} \geq 10$ nm (the center of the upper part of the TEM image in Fig. 1).

For each of the five agglomerates listed above, each of sections *1 – 4* in Fig. 4 shows the calculations of the distributions N/N_0 for LEF (Fig. 4*c*) and the probability density *w* of possible location points of RE ions (Fig. 4*d*) as a function of the distance *R* to the surface of the nearest Ag NP. The calculated LEF distributions and probability densities *w* of the possible location points of RE ions are averaged in all directions relative to the center of the particles. TEM images of the given groups of Ag NPs are shown in Fig. 4*a*, and the corresponding parts of the particle agglomerates (with only a portion of each agglomerate being presented) are shown in Fig. 4*b*. Section 4 (*c*) of Fig. 4 compares the LEF distributions calculated using Agglomerate-4 (*b1*, solid black curves) and Agglomerate-5 (*b2*, dotted blue curves). In section (*d*), probability density distributions of possible location points of RE ions corresponding to Agglomerate-4 (blue columns) and Agglomerate-5 (black columns) are compared. Table 1 shows the average enhancement of the LEF depending on the particle size *D*, the minimum distance between the particle centers R_{ij}, and the component composition of the NP. As shown in Figure 4 and Table 1, the LEF enhancement and the spatial distribution of these points relative to the nearest plasmonic NP are determined by the NP concentration, size, and degree of agglomeration. The lowest LEF enhancement effect, which varies insignificantly with increasing degree of agglomeration, is observed for particles smaller than 5 nm. This is due to the low scattering component present in the optical extinction spectrum of the sample, which determines the characteristics of LEF typical for small NPs. However, LEF increases with an increase in the size and degree of agglomeration for large NPs (≥ 10 nm) (Table 1). Moreover, at an identical concentration of Ag atoms in the particle state, the presence of small NPs (≤ 5 nm) along with relatively large NPs (≥ 10 nm, as in Agglomerate-5) leads to a noticeable decrease in the average LEF enhancement compared with glass having an insignificant number of small NPs (Agglomerate-4).

Based on the above considerations, the necessity of using larger NPs in order to achieve the maximum average LEF enhancement can be assumed. However, Fig. 5 shows that the field in the immediate vicinity of the Ag NPs increases with NP size only up to *D* of approximately 20 nm, followed by a decrease with larger sizes. A similar trend is observed for more distant areas from the NP surface; however, the limiting values of *D* at which the transition from increase to decrease in the LEF enhancement is observed are larger. Within an agglomerate of such NPs, the probability density of the possible locations of RE ions, being independent of their
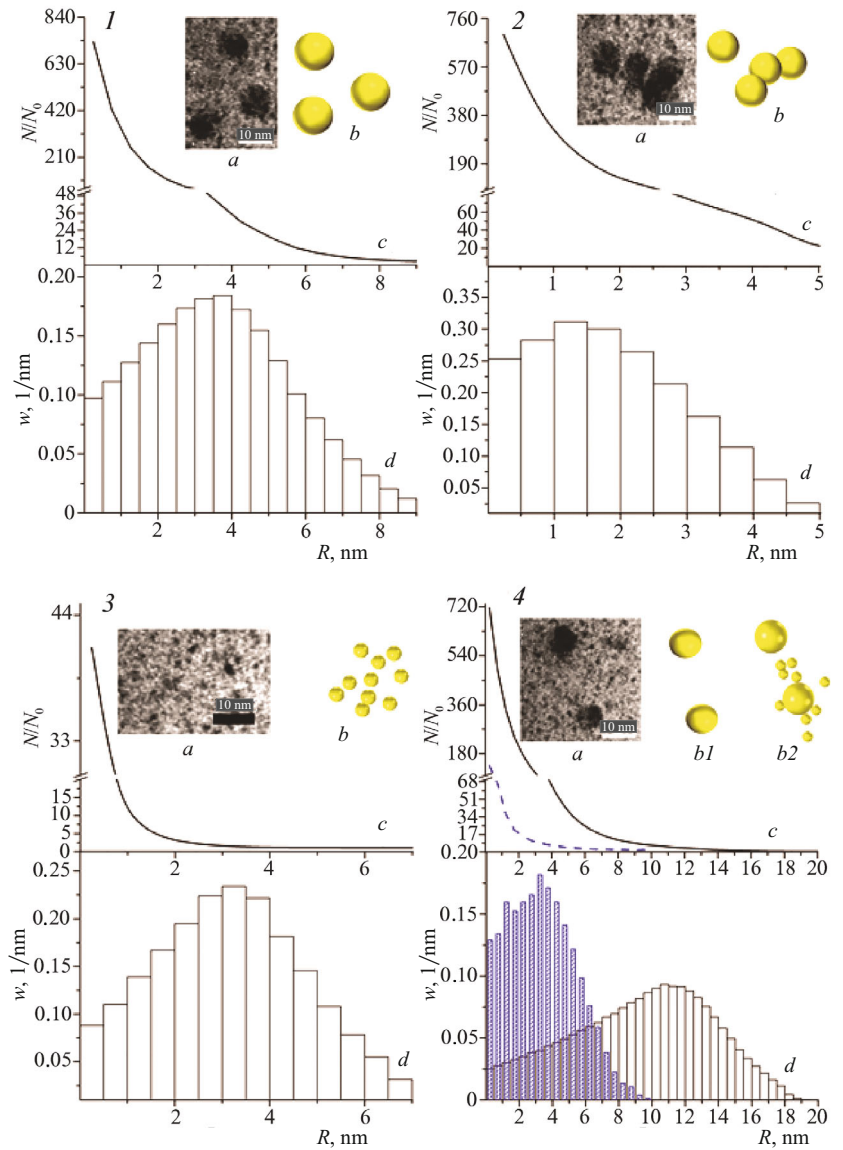
Fig. 4. Studied agglomerates (*a* and *b*), their characteristics (*d*), and optical properties (*c*).

concentration, exhibits a maximum at a certain distance. Therefore, for each NP agglomerate, an optimal particle size exists that provides the maximum average LEF enhancement.
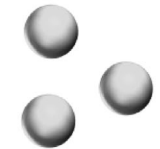
As mentioned above, the calculations disregarded the processes of concentration quenching [29] and the energy transfer from the RE ion to the nearest plasmonic NPs, which also leads to quenching of luminescence [47, 48]. The latter can result in a decrease in the LEF enhancement near the NP: the smaller the particle size, the stronger the quenching effect. In the present work, qualitative trends in the spatial distribution of LEF enhancement were identified, depending on the particle size and degree of their agglomeration. In order to verify the above estimate of the optimal size for plasmon particles obtained on the basis of a single-particle model, additional modeling was conducted to suggest the optimal sizes of silver nanoparticles and interparticle spacing within model agglomerates of identical particles.

In order to obtain quantitative structural parameter values for such an optimal configuration of silver nanoparticles, the interaction between the particles was considered. Here the average LEF enhancement per RE ion served as the enhancement criterion, taking into account the spatial volume between the nanoparticles. The modeling results showed that the highest LEF enhancement is characteristic of an Ag NP agglomerate having a size of approximately 25 nm and an average distance between the particle centers of approximately 30 nm.

CONCLUSIONS

Based on the study of the spatial distribution of LEF enhancement near silver plasmonic NPs and their agglomerates, along with the estimates of the average LEF enhancement at potential locations of the RE ion, the main conclusions are as follows:

TABLE 1. Average LEF Enhancement, Which Falls in One Point of the Hypothetical Location of RE Ion Near Various Agglomerates of Plasmonic Silver NPs at the Wavelength of Exciting Photons Corresponding to the Maximum LSPR for the Considered Agglomerate

No. of agglomerate	Fragment of NP agglomerate	Diameter D of NP, nm	Minimum distance R_{ij} between NP centers, nm	Wavelength of incident photon λ, nm	LEF enhancement per RE ion
1	Part of Agglomerate-1	10	15	440	117
2	Part of Agglomerate-2	10	12	440	242
3	Agglomerate-3	5	10	435	4.6
4	Part of Agglomerate-4	15	35	440	62
5	Agglomerate-5	15.5	17	425	33
6	Agglomerate-6	25	38	460	71
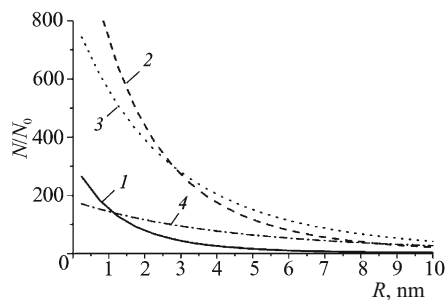
Fig. 5. N/N_0 distribution of LEF enhancement at distances R from the surface of single Ag NP having a size of $D = 15$ nm (*1*), $D = 20$ nm (*2*), $D = 30$ nm (*3*), and $D = 50$ nm (*4*).

– the proposed visual representation of the spatial distribution of the electric field near plasmon NP agglomerates ensures an effective comparative analysis of the field enhancement in hypothetical locations of RE ions;

– each of the considered local structural configurations of plasmon NP systems is quantitatively characterized by a corresponding average increase in the LEF intensity, which occurs at a hypothetical location of the RE ion in the immediate vicinity of the plasmon NP agglomerate;

– the enhancement of LEF intensity and the spatial distribution of such enhancement sites relative to the nearest plasmonic NP are determined by the NP concentration, size,

and degree of agglomeration, as well as the presence of small (≤ 5 nm) particles in the sample;

– the optimal configuration of silver nanoparticles in glass for obtaining the maximum average enhancement in the LEF intensity at the hypothetical locations of RE ions is an agglomerate of nanoparticles with sizes slightly exceeding 25 nm and average distances between the centers of particles of approximately 30 nm.

The mechanism presented in this work accounts for the intensity and spatial distribution of LEF near the agglomerates of plasmonic NPs that arises from excitation of LSPR. Such a mechanism is dominant in the enhancement of the luminescence of NPs with a size of ≥ 5 nm. An evaluation of the effects of interactions between the considered NPs and specific RE ions was beyond the scope of this study since the obtained estimates of the average LEF enhancement in the possible locations of the RE ion characterize the optical properties of the plasmon NP agglomerates. Therefore, the optimal concentration of RE ions in the sample remains unstudied. However, the maximum required concentration of RE ions (up to about 1.5 mol.% [29 – 31]), above which the concentration quenching of luminescence commences, can be assumed. Such concentrations of RE ions should lead neither to significant variations in the refractive index or the dielectric function of the glass [29] nor, consequently, to noticeable alterations in the characteristics of the LEF near the NPs and their agglomerates. Since the detailed interactions between RE ions and plasmonic NPs are beyond the scope of this work, additional studies will be required.

REFERENCES

1. C. D. Geddes, H. Cao, I. Gryczynski, et al., "Metal enhanced fluorescence (MEF) due to silver colloids on a planar surface: potential applications of indocyanine green to in Vivo imaging," *J. Phys. Chem. A.*, **107**(18), 3443 – 3449 (2003).

2. U. Kreibig and M. Vollmer, *Optical Properties of Metal Clusters*, Berlin, Heidelberg: Springer Berlin Heidelberg, **25**, 275 – 436 (1995).

3. B. N. S. Sooraj and T. Pradeep, "Optical properties of metal clusters," in: *Atomically Precise Metal Nanoclusters*, Elsevier (2023), pp. 83 – 101.

4. W. L. Barnes, A. Dereux, and T. W. Ebbesen, "Surface plasmon subwavelength optics," *Nature*, **424**(6950), 824 – 830 (2003).

5. S. Eustis and A. M. El-Sayed, "Why gold nanoparticles are more precious than pretty gold: Noble metal surface plasmon resonance and its enhancement of the radiative and nonradiative properties of nanocrystals of different shapes," *Chem. Soc. Rev. RSC*, **35**(3), 209 – 217 (2006).

6. P. Mulvaney, "Surface plasmon spectroscopy of nanosized metal particles," *Langmuir*, **12**(3), 788 – 800 (1996).

7. H. Yu, Y. Peng, Y. Yang, Z.-Y. Li, "Plasmon-enhanced light–matter interactions and applications," *NpjComput. Mater.*, **5**(1, 45 (2019).

8. M. I. Stockman, "Nanoplasmonics: past, present, and glimpse into future," *Opt. Express.*, **19**(22), 22029(2011).

9. Y. H. Su, W. H. Lai, L. G. Teoh, et al., "How the optical properties of Au nanoparticles are affected by surface plasmon resonance," in: *2006 IEEE International Conference on Semiconductor Electronics*, ICSE (2006), pp. 138 – 141.

10. J. R. Lakowicz, K. Ray, M. Chowdhury, et al., "Plasmon-controlled fluorescence: a new paradigm in fluorescence spectroscopy," *Analyst*, **133**(10), 1308 – 1346 (2008).

11. J.-F. Li, C.-Y. Li, and R. F. Aroca, "Plasmon-enhanced fluorescence spectroscopy," *Chem. Soc. Rev.*, **46**(13), 3962 – 3979 (2017).

12. Y. H. Jang, Y. J. Jang, S. Kim, et al., "Plasmonic solar cells: from rational design to mechanism overview," *Chem. Rev.*, **116**(24), 14982 – 15034 (2016).

13. D. M. Wu, A. García-Etxarri, A. Salleo, and J. A. Dionne, "Plasmon-enhanced upconversion," *J. Phys. Chem. Lett.*, **5**(22), 4020 – 4031 (2014).

14. J. Dong, W. Gao, Q. Han, et al., "Plasmon-enhanced upconversion photoluminescence: Mechanism and application," *Rev. Phys.*, **4**, 100026 (2019).

15. T. A. A. de Assumpção, L. R. P. Kassab, A. S. L. Gomes, et al., "Influence of the heat treatment on the nucleation of silver nanoparticles in Tm^{3+} doped $PbO–GeO_2$ glasses," *Appl. Phys. B*, **103**(1), 165 – 169 (2011).

16. B. N. Swetha, K. Keshavamurthy, and G. Jagannath, "Influence of size of Ag NP on spectroscopic performances of Eu^{3+} ions in sodium borate glass host," *Optik (Stuttg).*, **240**, 166918 (2021).

17. B. N. Swetha, K. Keshavamurthy, G. Gupta, et al., "Silver nanoparticles enhanced photoluminescence and the spectroscopic performances of Nd^{3+} ions in sodium lanthanum borate glass host: Effect of heat treatment," *Ceram. Int.*, **47**(15), 21212 – 21220 (2021).

18. H. Fares, W. Stambouli, H. Elhouichet, et al., "Nanosilver enhanced luminescence of Er3+ ions embedded in tellurite glass, vitro-ceramic and ceramic: impact of heat treatment," *RSC Adv.*, **6**(37), 31136 – 31145 (2016).

19. T. Som and B. Karmakar, "Surface plasmon resonance in nano-gold antimony glass-ceramic dichroic nanocomposites: One-step synthesis and enhanced fluorescence application," *Appl. Surf. Sci.*, **255**(23), 9447 – 9452 (2009).

20. W. Zhang, J. Lin, M. Cheng, et al., "Radiative transition, local field enhancement and energy transfer microcosmic mechanism of tellurite glasses containing Er^{3+}, Yb^{3+} ions, and Ag nanoparticles," *J. Quant. Spectrosc. Radiat. Transf.*, **159**, 39 – 52 (2015).

21. Z. Ashur Said Mahraz, M. R. Sahar, S. K. Ghoshal, et al., "Silver nanoparticles enhanced luminescence of Er^{3+} ions in borotellurite glasses," *Mater. Lett.*, **112**, 136 – 138 (2013).

22. J. A. Scholl, A. L. Koh, and J. A. Dionne, "Quantum plasmon resonances of individual metallic nanoparticles," *Nature*, **483**(7390), 421 – 427 (2012).

23. X. Zhang, C. A. Marocico, M. Lunz, et al., "Experimental and theoretical investigation of the distance dependence of localized surface plasmon coupled F?rster resonance energy transfer," *ACS Nano*, **8**(2), 1273 – 1283 (2014).

24. J. Zhang, Y. Fu, and J. R. Lakowicz, "Enhanced Forster resonance energy transfer (FRET) on a single metal particle," *J. Phys. Chem. C*, **111**(1), 50 – 56 (2007).

25. O. P. Chikalova-Luzina, A. N. Aleshin, and I. P. Shcherbakov, "Specific features of energy transfer in nanocomposite films

based on MEH-PPV polymer semiconductor and ZnO nano-particles," *Phys. Solid State*, **57**(3), 618 – 623 (2015).

26. A. Govorov, P. L. Hernández Martínez, and H. V. Demir, *Understanding and Modeling Förster-Type Resonance Energy Transfer (FRET)*, Springer Singapore, Singapore (2016).

27. T. Som and B. Karmakar, "Enhanced frequency upconversion of Sm^{3+} ions by elliptical Au nanoparticles in dichroic Sm^{3+}: Au antimony glass nanocomposites," *Spectrochim. Acta, Part A, Mol. Biomol. Spectrosc.*, **75**(2), 640 – 646 (2010).

28. C. Yu, Z. Yang, J. Zhao, et al., "Preparation and photoluminescence enhancement of Au nanoparticles with ultra-broad plasmonic absorption in glasses," *J. Am. Ceram. Soc.*, **102**(7), 4200 – 4212 (2019).

29. S. Dai, C. Yu, G. Zhou, et al., "Concentration quenching in erbium-doped tellurite glasses," *J. Lumin.*, **117**(1), 39 – 45 (2006).

30. K. Kumar, S. B. Rai, and D. K. Rai, "Upconversion and concentration quenching in Er^{3+}-doped TeO_2–Na_2O binary glasses," *J. Non. Cryst. Solids*, **353**(13 – 15), 1383 – 1387 (2007).

31. W. Zhang, J. Lin, G. Sun, et al., "Stability, glass forming ability and spectral properties of Ho/Yb co-doped TeO_2–WO_3–Zn_X ($X = O/F_2/Cl_2$) system," *Opt. Mater.* (Amst), **36**(6), 1013 – 1019 (2014).

32. M. Heinz, V. V. Srabionyan, A. L. Bugaev, et al., "Formation of silver nanoparticles in silicate glass using excimer laser radiation: Structural characterization by HRTEM, XRD, EXAFS, and optical absorption spectra," *J. Alloys Compd.*, **681**, 307 – 315 (2016).

33. M. Heinz, V. V. Srabionyan, L. A. Avakyan, et al., "Formation and implantation of gold nanoparticles by ArF-excimer laser irradiation of gold-coated float glass," *J. Alloys Compd.*, **736**, 152 – 162 (2018).

34. M. Heinz, V. V. Srabionyan, L. A. Avakyan, et al., "Formation of bimetallic gold-silver nanoparticles in glass by UV laser irradiation," *J. Alloys Compd.*, **767**, 1253 – 1263 (2018).

35. A. S. Lipatiev, S. S. Fedotov, S. V. Lotarev, et al., "Single-pulse laser-induced Ag nanoclustering in silver-doped glass for high-density 3D-rewritable optical data storage," *ACS Appl. Nano Mater.*, **5**(5), 6750 – 6756 (2022).

36. G. Shakhgildyan, V. Durymanov, M. Ziyatdinova, et al., "Effect of gold nanoparticles on the crystallization and optical proper-ties of glass in ZnO–MgO–Al_2O_3–SiO_2 system," *Crystals*, **12**(2), 287 (2022).

37. V. V. Srabionyan, L. A. Avakyan, V. A. Durymanov, et al., "Atomic structure and optical properties of color centers of silver in AgAu/glass irradiated by UV laser," *J. Phys. Chem. Solids.*, **179**, 111412 (2023).

38. V. V. Srabionyan, M. Heinz, S. Y. Kaptelinin, et al., "Effect of thermal post-treatment on surface plasmon resonance characteristics of gold nanoparticles formed in glass by UV laser irradiation," *J. Alloys Compd.*, **803**, 354 – 363 (2019).

39. D. W. Mackowski and M. I. Mishchenko, "A multiple sphere T-matrix Fortran code for use on parallel computer clusters," *J. Quant. Spectrosc. Radiat. Transf.*, **112**(13), 2182 – 2192 (2011).

40. L. A. Avakyan, *Python Wrapper for Multiple Sphere T-matrix (MSTM) Code to Calculate Surface Plasmon Resonance (SPR) Spectrum* (2017). URL: https://github.com/lavakyan/mstm_spectrum

41. L. A. Avakyan, M. Heinz, A. V. Skidanenko, et al., "Insight on agglomerates of gold nanoparticles in glass based on surface plasmon resonance spectrum: study by multi-spheres T-matrix method," *J. Phys. Condens. Matter.*, **30**(4), 045901 (2018).

42. *COMSOL Multiphysics® v. 5.6*, COMSOL AB, Stockholm, Sweden. URL: www.comsol.com

43. J.-P. Berenger, "A perfectly matched layer for the absorption of electromagnetic waves," *J. Comput. Phys.*, **114**(2), 185 – 200 (1994).

44. H. U. Yang, J. D'Archangel, M. L. Sundheimer, et al., "Optical dielectric function of silver," *Phys. Rev. B*, **91**(23), 235137 (2015).

45. J. M. J. Santillán, F. A. Videla, M. B. Fernández van Raap, et al., "Influence of size-corrected bound-electron contribution on nanometric silver dielectric function. Sizing through optical extinction spectroscopy," *J. Phys. D. Appl. Phys.*, **46**(43), 435301 (2013).

46. J. R. Lakowicz, "Radiative decay engineering 5: metalenhanced fluorescence and plasmon emission," *Anal. Biochem.*, **337**(2), 171 – 194 (2005).

47. G. Y. Shakhgildyan, S. Lotarev, and M. Vetchinnikov, "Thermally-induced precipitation of gold nanoparticles in phosphate glass: effect on the optical properties of Er^{3+} ions," *J. Non. Cryst. Solids.*, **550**, 120408 (2020).